PHYSICAL REVIEW E **77**, 041906 (2008)

Anomalous diffusion of a tethered membrane: A Monte Carlo investigation

Hristina Popova and Andrey Milchev
Institute of Physical Chemistry, Bulgarian Academy of Sciences, 1113 Sofia, Bulgaria

(Received 17 September 2007; published 15 April 2008)

Using a continuum bead-spring Monte Carlo model, we study the anomalous diffusion dynamics of a self-avoiding tethered membrane by means of extensive computer simulations. We focus on the subdiffusive stochastic motion of the membrane's central node in the regime of flat membranes at temperatures above the membrane folding transition. While at times, larger than the characteristic membrane relaxation time τ_R, the mean-square displacement of the center of mass of the sheet, $\langle R_c^2 \rangle$, as well as that of its central node, $\langle R_n^2 \rangle$, show the normal Rouse diffusive behavior with a diffusion coefficient D_N scaling as $D_N \propto N^{-1}$ with respect to the number of segments N in the membrane, for short times $t \le \tau_R$ we observe a *multiscale dynamics* of the central node, $\langle R_n^2 \rangle \propto t^\alpha$, where the anomalous diffusion exponent α changes from $\alpha \approx 0.86$ to ≈ 0.27, and then to $\alpha \approx 0.5$, before diffusion turns eventually to normal. By means of simple scaling arguments we show that our main result, $\alpha \approx 0.27$, can be related to particular mechanisms of membrane dynamics which involve different groups of segments in the membrane sheet. A comparative study involving also linear polymers demonstrates that the diffusion coefficient of self-avoiding tethered membranes, containing N segments, is three times smaller than that of linear polymer chains with the same number of segments.

DOI: 10.1103/PhysRevE.77.041906 PACS number(s): 87.16.D−, 02.50.Ey, 87.15.A−, 87.15.Vv

I. INTRODUCTION

There has been considerable interest recently in understanding the statistical properties of polymerized (or tethered) membranes [1]. This interest in large part is due to the membrane behavior which is much richer than that of polymers, their one-dimensional analog. In addition, this interest is justified by a variety of real systems like red-blood-cell cytoskeletons [2], graphite oxide sheets [3,4] or dispersed silicate (clay) platelets [5,6] which can be modeled by networks of fixed connectivity, generally referred to as polymerized membranes. Along with the experimental studies, self-avoiding polymerized membranes have also attracted remarkable interest from the point of view of basic research in recent years. Their static properties have been studied analytically and numerically [7–19]. Much of these studies have been spent in the pursuit of the so called "crumpling transition" between a low-temperature flat phase and a high-temperature crumpled phase until it was realized [14,20,21] that self-avoiding membranes are always flat (with an *infinite* persistence length), i.e., their radius of gyration R_g scales with linear size L as $R_g \propto L^\nu$ where the Flory exponent $\nu \approx 1$. The flat phase arises even without explicit bending rigidity because the resistance to in-plane shear deformations leads to anomalous stiffening of the surface in the presence of thermal fluctuations.

In contrast to static properties, the membrane dynamics is less well-understood. Earlier analytical and numeric studies [7,13,22,23] have revealed that the self-avoiding restrictions considerably modify the relaxation times of the tethered surface. Thus the typical relaxation time τ_R of a tethered membrane in the case of Rouse dynamics when hydrodynamic interactions are neglected has been predicted by simple scaling arguments [7] to vary as $\tau_R \propto L^{2+2\nu} \propto R_g^{2+2/\nu}$. If, as in polymer physics, one introduces a *dynamic exponent* z, describing the relaxation process as $\tau_R \propto R_g^z$, then one gets $z = 2 + 2/\nu$ (for linear polymers one has $z = 2 + 1/\nu$). Usually, τ_R is considered to be the time needed for the membrane to diffuse its radius of gyration. For tethered membranes, highly permeable to the solvent as in isolated spectrin networks, one is in the Rouse regime [22] and the diffusion coefficient D_N scales with membrane size L as $D_N \propto L^{-2}$. Thus the time it takes for such a flat membrane to move a distance R_g is proportional to L^4. In contrast, for impermeable membranes (like, e.g., erythrocytes) where solvent backflow (i.e., a long-ranged hydrodynamic interaction) is important, one has in d-dimensions in the case of Zimm dynamics $\tau_H \propto R_g^d \propto L^{d\nu}$ (i.e., $z = d$) and $D_N \propto L^{-1}$. Thus one may view permeability as constituting two different dynamic universality classes of tethered membranes [22] whereby these classes (Rouse dynamics—highly permeable membranes, or Zimm dynamics—impermeable membranes) are observed for a wave vector independent (or, dependent) friction coefficient. Recently, a series of simulation studies by Pandey *et al.* [24,25] has revealed a multiscale stochastic dynamics of tethered membranes at times before normal diffusive behavior is reached. The displacement motion of the central node, R_n, of a four-coordinated coarse-grained model membrane has been observed to undergo a subdiffusive mean-square displacement (MSQD) $\langle R_n^2 \rangle \propto t^\alpha$ with the exponent α attaining different values in the short and intermediate time regimes before turning to normal diffusion for $t \ge \tau_R$ with $\alpha = 1$.

In the present work we employ an efficient off-lattice Monte Carlo algorithm, focusing on the subdiffusive dynamics of self-avoiding tethered membranes and comparing some of the salient dynamic features to those of linear polymers. Our observations, based on extensive computer simulations, largely confirm those of previous investigators [24,25]. As a step forward, however, we suggest a scaling theory which explains our findings for the anomalous membrane dynamics, relating the observed values of α to the specific stochastic motion of particular groups of sheet segments.

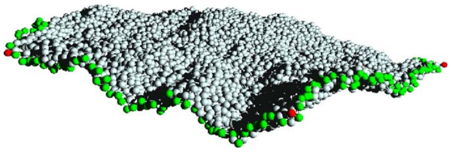

FIG. 1. (Color online) A snapshot of a tethered membrane at $T=1.0$ with linear size (the edge length of a regular hexagonal sheet) $L=50$ which contains $N=7351$ monomers. Periphery segments at the rim of the membrane are shaded gray (green) while the six monomers at the vertices (corners) of the sheet are dark gray (red).

After briefly introducing our model in Sec. II, this is considered in Sec. III where we focus on the main results of our investigation and their interpretation. We close this paper with a brief summary and discussion in Sec. IV.

II. MODEL SYSTEM AND SIMULATION PROCEDURE

We study a coarse-grained model of *self-avoiding tethered membranes*, embedded in three-dimensional space. The membranes have a hexagonal lattice structure where each monomer interacts with six nearest-neighbors—Fig. 1. There are altogether $N=(3L^2-3L+1)$ monomers in such a membrane where by L we denote the number of monomers on the edge of the network (i.e., L is the linear size of the membrane). In this model, spherical particles of diameter σ are connected in a fixed geometry by flexible strings of length l. To prevent self-intersection of the membrane, the maximum length of the strings between the centers of the spheres must be $l\leq\sqrt{3}\sigma$, then the membrane is self-avoiding in that it cannot intersect itself.

The bonded nearest-neighbor monomers on the membrane interact with each other through the finitely extensible nonlinear elastic (FENE) potential [26] where a bond l has a maximum length $l_{\max}$ and a minimum length $l_{\min}$,

$$U_{\mathrm{FENE}}(l)=-K(l_{\max}-l_0)^2\ln\left[1-\left(\frac{l-l_0}{l_{\max}-l_0}\right)^2\right]. \qquad (1)$$

The minimum of this potential occurs for $l=l_0$, $U_{\mathrm{FENE}}(l_0)=0$, near l_0 it is harmonic, with K being a spring constant, and the potential diverges to infinity both when $l\to l_{\max}$ and when $l\to l_{\min}$. Choosing our length unit $l_{\max}=1.0$, we choose the other parameters as $l_{\min}=0.2$, $l_0=(l_{\min}+l_{\max})/2=0.6$, and $K/k_BT=5$, where T denotes the absolute temperature, and k_B is the Boltzmann constant.

Self-avoidance is observed by the interaction between particles which are not nearest neighbors on the network. The nonbonded interaction between monomers is described by a Morse potential where r is the distance between the monomers,

$$U_{\mathrm{Morse}}(r)/\epsilon_M=\exp[-2\alpha(r-r_{\min})]-2\exp[-\alpha(r-r_{\min})] \qquad (2)$$

with parameters $\epsilon_M/k_BT=1$ and $\alpha=24$. The minimum of this potential occurs for $r=r_{\min}$ and $U_{\mathrm{Morse}}(r_{\min})/\epsilon_M=-1$. For $\alpha=24$, $U_{\mathrm{Morse}}(r)$ essentially is zero for $r\geq1.25r_{\min}$. Choosing then units of length such that $r_{\min}=0.8$, we hence can take $U_{\mathrm{Morse}}(r\geq1)=0$. The repulsive part of this potential guarantees self-avoidance of the membrane.

We have used the standard Monte Carlo procedure to investigate the thermodynamic properties of self-avoiding tethered membranes. The total energy (Hamiltonian) is the sum of Eqs. (1) and (2). In each Monte Carlo update, a monomer is chosen at random and one attempts to displace it randomly by displacements chosen uniformly from the intervals $-0.25\leq\Delta x$, Δy, $\Delta z\leq+0.25$. The attempted move is accepted or rejected according to the conventional Metropolis criterion by comparing the transition probability $W=\exp(-\Delta U/k_BT)$ (where ΔU is the energy difference between the configurations after and before the trial move) with a random number uniformly distributed between zero and unity. If W exceeds this random number, the attempted move is accepted, otherwise it is rejected. Time is measured in Monte Carlo steps (MCS) per monomer whereby a single MCS is elapsed after N monomers are picked at random and given the chance to perform a trial move. Since our potentials are constructed such that the membrane cannot intersect itself in the course of random displacements of monomers, one does not need to check separately for entanglement restrictions during the simulation. Thus the algorithm is reasonably fast. Nevertheless, the simulation takes quite a long time for large self-avoiding membranes to equilibrate and then move a substantial distance in space. This and the necessity to attain very good statistical accuracy have limited our investigations to sizes $L\leq50$. Eventually, we would like to note that the interactions used in the present off-lattice model, albeit somewhat more refined and complicated than the simple potential used in earlier simulations on a cubic lattice [24,25], do not change the physics of the problem and lead qualitatively to the same results.

III. RESULTS

Before we focus on the subdiffusive dynamics of our membranes, we show in Fig. 2 the scaling behavior of the gyration radius,

$$\langle R_g^2\rangle=\frac{1}{N}\sum_{i=1}^{N}\langle(r_i-r_{cm})^2\rangle, \qquad (3)$$

where r_i is the position of the ith monomer of the membrane while $r_{cm}=\frac{1}{N}\sum_{i=1}^{N}r_i$ is its center-of-mass location. We also sample the eigenvalues $\lambda_{\max}^2$, λ_{med}^2, and $\lambda_{\min}^2$ of the inertial tensor,

$$I_{\alpha\beta}=\frac{1}{N}\sum_{i=1}^{N}(r_i^{\alpha}-r_{cm}^{\alpha})(r_i^{\beta}-r_{cm}^{\beta}), \qquad (4)$$

where $\alpha,\beta\in\{x,y,z\}$, the sum is taken over all particles of a given configuration, and r_{cm}^{α} is the α component of the center-of-mass radius vector for a given configuration. The three eigenvalues are ordered according to magnitude $\lambda_{\max}^2\geq\lambda_{\mathrm{med}}^2\geq\lambda_{\min}^2$. The directions of the principal axes are given by the three eigenvectors corresponding to the three eigenvalues. For a planar membrane, the eigenvector associ-

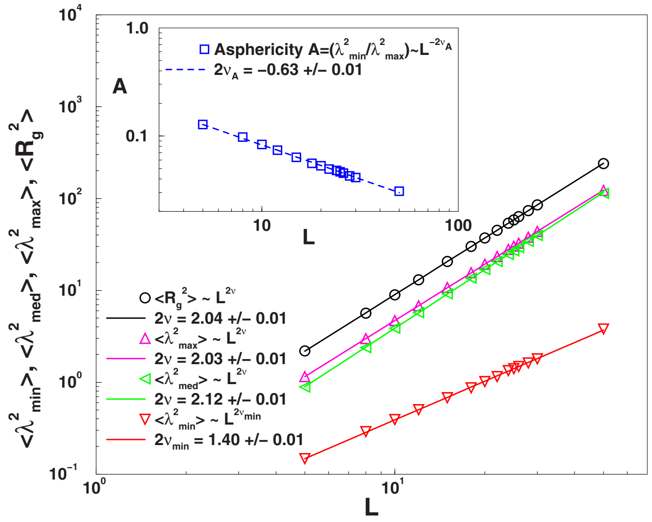

FIG. 2. (Color online) Log-log plot of the mean-squared radius of gyration, R_g^2, and the three eigenvalues, $\lambda^2_{\rm max}$, $\lambda^2_{\rm med}$, and $\lambda^2_{\rm min}$ against the linear size L of flat tethered membranes ($5 \le L \le 50$) at $T=1.0$. The respective exponents are given in the legend. In the inset we show the variation of membrane asphericity, $A=\lambda^2_{\rm min}/\lambda^2_{\rm max}$ which vanishes with L as $A \propto L^{-0.63}$.

ated with $\lambda^2_{\rm min}$ is perpendicular to the plane of the membrane while the eigenvectors associated with $\lambda^2_{\rm max}$ and $\lambda^2_{\rm med}$ lie in the plane of the membrane. It is evident from Fig. 2 that our membranes are indeed flat with scaling exponents $\nu=1.02\pm0.01$ for R_g, $\nu=1.02\pm0.01$ for $\lambda^2_{\rm max}$, and $\nu=1.06\pm0.01$ for $\lambda^2_{\rm med}$. The asphericity ratio $A=(\lambda^2_{\rm min}/\lambda^2_{\rm max})\propto L^{-2\nu_A}$ tends to zero with an exponent $\nu_A=0.32\pm0.01$, indicating that these membranes are indeed asymptotically flat. Note that these data have been obtained at $T=1.0$ well above the temperature of the first folding transition [27], $T_{c_1}=0.89\pm0.01$. In Fig. 2 and in the following figures the error bars do not exceed the size of the symbols.

Turning now to membrane dynamics in the Rouse regime, one may assume that each segment of the membrane moves under the influence of surface forces (surface stretching due to near-neighbors and excluded volume forces due to distant neighbors), and a random force representing thermal noise. As far as the contribution of inertial terms to membrane motion can be neglected for sufficiently long times, one may assume that the relevant dynamics is purely diffusive. With ρ being the rate of position changes of monomers per unit time and $z=2/\nu+2$, the dynamic exponent, one may write the relaxation time of the membrane τ_R as

$$\tau_R=\rho^{-1}R_g^z=\rho^{-1}N^{z\nu/2}. \tag{5}$$

If monomeric orientations add up randomly and one neglects correlations, the MSQD of the membrane center of mass is

$$g_3(t)=\langle[\vec{r}_{cm}(t)-\vec{r}_{cm}(0)]^2\rangle=\rho\left\langle\left(\frac{l}{N}\right)^2\right\rangle Nt=\rho\frac{\langle l^2\rangle}{N}t, \tag{6}$$

because each monomeric motion moves the center of mass by a random displacement of the order l/N, l being the bond length. There are ρN such random motions per unit time. Invoking the Einstein relation $g_3(t)=2dD_Nt$ (where d is the spatial dimensionality), one thus concludes

$$D_N \propto \rho\langle l^2\rangle/N. \tag{7}$$

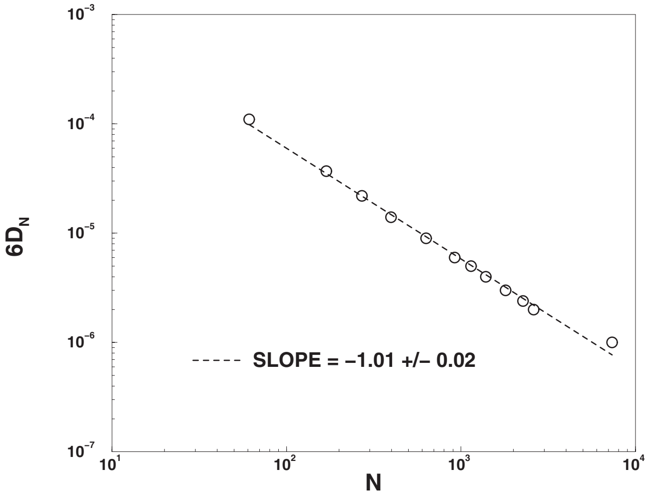

FIG. 3. Variation of the diffusion coefficient D_N of a membrane with the number of monomers N for membrane sizes $5\le L\le 50$ at $T=1.0$. The measured slope is -1.01 ± 0.02.

From Fig. 3 it is evident that this prediction, Eq. (7), is indeed nicely confirmed by the simulation. The relaxation time τ_R and the scaling law $z\nu=2\nu+2$ is then understood by the condition that the membrane is relaxed when its center of mass has diffused over its own size R_g, i.e.,

$$g_3(\tau_R)\propto\rho\frac{\langle l^2\rangle}{N}\tau_R\propto\langle l^2\rangle N^{z\nu/2-1}\propto R_g^2\propto\langle l^2\rangle N^\nu, \tag{8}$$

whence $z\nu=2+2\nu$ follows.

These arguments can be carried over for the MSQD of the membrane central node as well. We define

$$g_1(t)=\langle[\vec{r}_n(t)-\vec{r}_n(0)]^2\rangle\propto\langle l^2\rangle(\rho t)^\alpha \tag{9}$$

at time $t<\tau_R$ anticipating that the central node exhibits anomalous diffusion with an exponent $\alpha<1$. For short times $(\rho t)\le 1$, of course, a nearly free diffusion of the central node takes place, and thus $g_1(t)$ for $\rho t\approx 1$ should be of the order of $\propto\langle l^2\rangle$. Requiring now that $g_1(\tau_R)\approx R_g^2$, one gets a scaling relation for α,

$$g_1(\tau_R)\propto\langle l^2\rangle(\rho\tau_R)^\alpha\propto\langle l^2\rangle N^{\alpha z\nu/2}\propto\langle l^2\rangle N^\nu. \tag{10}$$

Thus for flat membranes with $\nu=1$, one has $\alpha^{-1}=1+\nu^{-1}=2$, and one would then expect to see a time interval $t<\tau_R$ where $g_1(t)\propto t^{1/2}$. Additional information for the subdiffusive dynamics of the membrane may be obtained if one defines in analogy with the case of linear polymers [28] the MSQD of a central node measured in the center-of-mass coordinate system of the membrane,

$$g_2(t)=\langle[\vec{r}_n(t)-\vec{r}_{cm}(t)-\vec{r}_n(0)+\vec{r}_{cm}(0)]^2\rangle, \tag{11}$$

and also for the averaged MSQD of the six monomers at the vertices of the hexagonal sheet in the laboratory system of coordinates,

$$g_4(t) = \left\langle \frac{1}{6}\sum_{i=1}^{6} [\vec{r}_i(t) - \vec{r}_i(0)]^2 \right\rangle . \tag{12}$$

In the center-of-mass coordinate system of the membrane,

$$g_5(t) = \left\langle \frac{1}{6}\sum_{i=1}^{6} [\vec{r}_i(t) - \vec{r}_{cm}(t) - \vec{r}_i(0) + \vec{r}_{cm}(0)]^2 \right\rangle . \tag{13}$$

Evidently, for $t < \tau_R$ one should observe $g_2(t) \approx g_1(t)$ and $g_5(t) \approx g_4(t)$ whereas $g_2(t) \propto R_g^2$ for $t \gg \tau_R$ since the central monomer cannot travel farther from the center of mass than the membrane size, of course.

A general impression about the time variation of the various MSQD $g_i(t)$ and the similarity in the stochastic dynamics of linear polymers and tethered membranes may be gained from Fig. 4. It is seen that the course of the functions g_i with time is qualitatively very similar for both linear polymers and tethered membranes. In both cases, cf. Figs. 4(a) and 4(b), one finds that the center of mass performs normal diffusion with $g_3(t) = 6D_N t$. One can, therefore, compare the relative diffusivity of polymers and membranes, containing the *same* number of monomers N, say a chain with $N=256$ and a membrane with $L=10$, i.e., $N=271$, with identical forces acting between the repeating units. Our analysis shows that in a good solvent, $T=1.0$, one obtains $6D_N(\text{polymer}) = 6.6\times 10^{-5}$ and $6D_N(\text{membrane}) = 2.2\times 10^{-5}$, i.e., a linear self-avoiding chain of N segments moves *three times faster* than a self-avoiding flat sheet in the case of Rouse dynamics. We find this result rather remarkable since this decrease in mobility is solely and entirely due to the higher topological dimensionality of the membrane.

A marked difference between chains and membranes, however, is revealed if one looks at the subdiffusive behavior of the central monomer in both cases. For times shorter than the typical relaxation time, $t < \tau_R$, the central node of the polymer chain is observed to diffuse like $g_1(t) \propto t^{0.58}$ (i.e., very close to the expected $t^{0.54}$ power law) while for the membrane one finds a much smaller power $g_1(t) \propto t^{0.3}$, seen also by Pandey *et al.* [25]. It might be argued that this small exponent $\alpha \approx 0.3$, describing the subdiffusive behavior of a tethered membrane, reflects a membrane-specific dynamic mechanism which shows up at $t < \tau_R$. In the following we suggest a possible interpretation and a simple scaling derivation for the observed value of this exponent α.

We first look more closely at the main data of our study showing the MSQD of the central monomer of a tethered membrane in Fig. 5. The different regimes of subdiffusive motion of the central node are indicated by power laws with exponents, specified in the legend of Fig. 5. It is seen that for very short time, $0 < t \leq 1$, each segment indeed performs displacements which are not constrained by the topological connectivity of the network so with $g_1(t) \propto t^{0.86}$ one observes an extremely shortlived nearly normal diffusion. At late times, $t \geq \tau_R$, the normal diffusive motion sets on eventually, and $g_1(t) \approx g_3(t) \propto 6D_N t$. We should like to point out that at late times the averaging of the correlation functions g_1 for the two largest system sizes, $L=30-50$, is not perfect due to a progressively deteriorating statistics, however, it is beyond doubt that their ultimate slope corresponding to normal diffusion should be unity. In the intermediate time interval our data yields a subdiffusive motion of the central monomer with $g_1(t) \propto t^{\alpha}$ where $\alpha = 0.27 \pm 0.01$. Due to strong finite-size effects this value of the α can be unambiguously established for sufficiently large, $20 \leq L \leq 50$ membranes only. We note that very close values for $\alpha \approx 0.25-0.32$ have been observed recently in the computer experiments of Pandey *et al.* [25] for the case of tethered membranes in the good solvent regime at temperatures $2.0 \leq T \leq 10$. Such behavior cannot be explained by means of the exponent $\alpha = 0.5$ which follows from the estimate, Eq. (10).

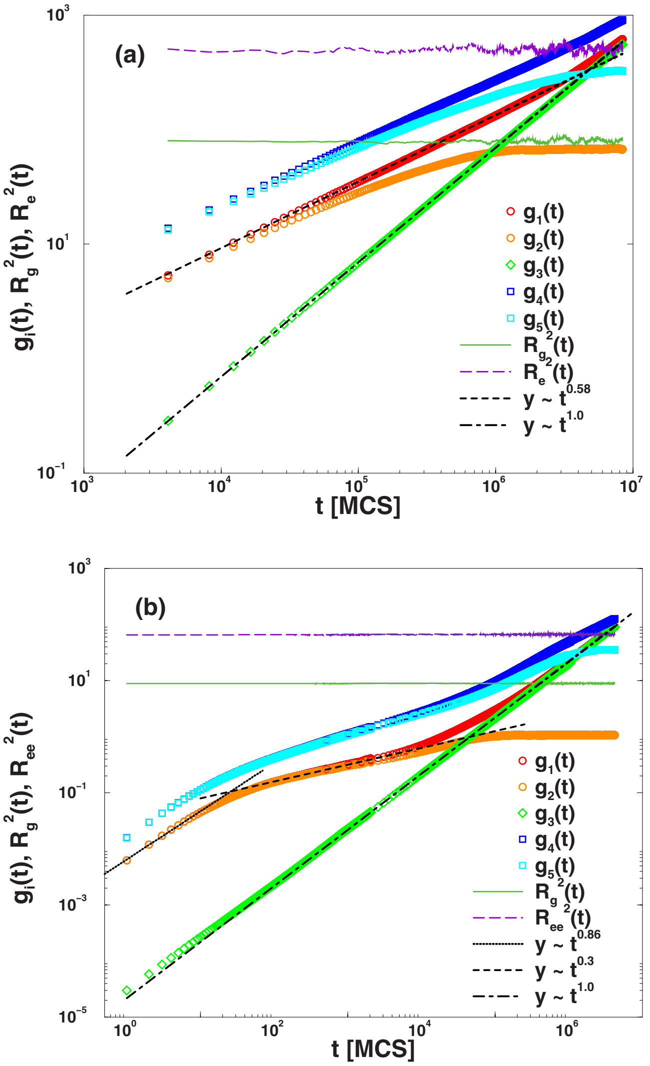

FIG. 4. (Color online) Log-log plot of mean-square displacements $g_1(t)$, $g_2(t)$, $g_3(t)$, $g_4(t)$, and $g_5(t)$ at $T=1.0$ plotted vs time t (measured in Monte Carlo steps) for a linear polymer of length $N=256$ (a), and for a membrane of size $L=10$ which contains $N=271$ monomers (b). Dashed lines indicate the scaling behavior of the central segment MSQD, $g_1(t) \propto t^{\alpha}$, and of the center of mass, $g_3(t) \propto t$, with elapsed time while horizontal lines denote the time averages of the radius of gyration R_g^2 and of the "end-to-end" distance of the chain, R_e^2 (a), and of the membrane, R_{ee}^2 (b), the latter being measured as the distance between the opposite vertices of the hexagonal sheet. Evidently, cf. (b), by defining τ_R from $g_3(\tau_R) = R_g^2$ as the mean relaxation time of the membrane one can verify that $g_1(\tau_R) \approx g_3(\tau_R)$.

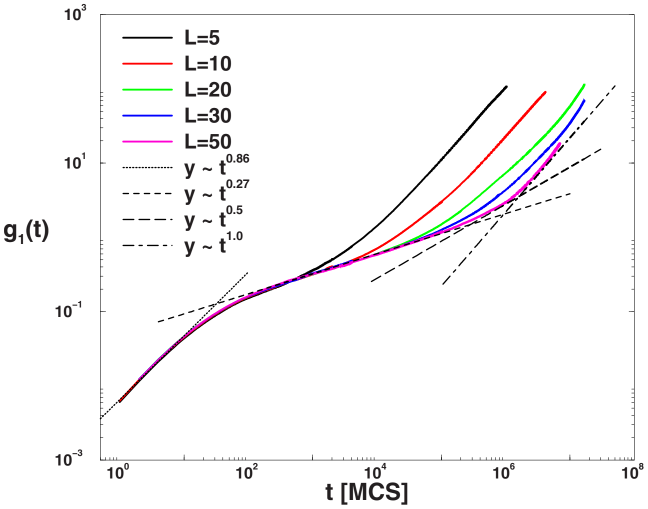

FIG. 5. (Color online) Log-log plot of the central node MSQD g_1 vs time t at $T=1.0$ for a membranes with linear size $5 \leq L \leq 50$. All data are averaged over 100 simulation runs. Dashed lines denote power law variation with different exponents (see legend) corresponding to the various subdiffusive regimes.

We believe that a possible explanation of this sluggishness of flat membranes at early times $1 < t \leq \tau_1 < \tau_R$ may be found if one assumes that in this interval only the most loosely bound monomers (those at the membrane periphery, or rather, those at the six vertices of the hexagonal sheet) actually contribute to a displacement of the membrane center of mass while all monomers with sixfold coordination in the bulk of the membrane are virtually blocked by their neighbors and for this short time hardly move. As far as the membrane retains its flat shape and does not fold, the maximal displacement of these loosely bound monomers cannot exceed the effective thickness λ_{min}. Indeed, a comparison of Figs. 2 and 5 shows that the MSQD, performed by a membrane of linear size L during the time τ_1 (the latter is given by the intersection point of the tangent $y \propto t^{\alpha}$ to g_1, and $g_3 \propto t$) amounts to $g_3(\tau_1) \approx \lambda_{\text{min}}^2$. One can, therefore, estimate the characteristic time τ_1 if, in analogy to Eq. (6), one considers

$$g_3(t) = \rho \left\langle \left(\frac{l}{N} \right)^2 \right\rangle \sqrt{N} t, \tag{14}$$

in case that *only* the membrane periphery of length $\propto \sqrt{N}$ contributes to the center-of-mass displacement. Thus during $1 < t \leq \tau_1$ the diffusion coefficient of the membrane becomes $D \propto N^{-3/2} \propto L^{-3}$ reflecting the slow displacement of the center of mass. Equation (14) therefore suggests $\tau_1 \propto L^{3+2\nu_{\text{min}}} \approx L^{4.4}$. With $g_1(\tau_1) \propto L^{\alpha(3+2\nu_{\text{min}})} \approx \lambda_{\text{min}}^2$ one obtains then the broken exponent for a *periphery-driven* membrane $\alpha_p = (2\nu_{\text{min}})/(3+2\nu_{\text{min}}) = 0.32$.

In contrast, if only a finite number of loosely bound monomers at the vertices effect the net displacement of the center of mass, one obtains then

$$g_3(t) = \rho \left\langle \left(\frac{l}{N} \right)^2 \right\rangle t, \tag{15}$$

and therefore temporarily $D \propto N^{-2} \propto L^{-4}$ so that $\tau_1 \propto L^{4+2\nu_{\text{min}}} \approx L^{5.4}$. In this case one gets the exponent for anomalous diffusion of a *vertices-driven* membrane $\alpha_v = (2\nu_{\text{min}})/(4+2\nu_{\text{min}}) = 0.26$.

Thus we obtain two estimates which may be considered as the lower and upper bounds of the anomalous diffusion exponent, $\alpha_v \leq \alpha \leq \alpha_p$, depending on the particular mechanism involved in the diffusive motion. The measured value of $\alpha \approx 0.27$ lies indeed within these limits. Of course, one should bear in mind that most probably neither mechanism of diffusion (vertices-driven or periphery-driven) takes place alone and the real process involves a mixture of both. Moreover, at this point we cannot rule out the possibility that at times $\tau_1 \leq t \leq \tau_R$ *all* membrane segments eventually get the chance to perform an elementary move and thus contribute to the center-of-mass motion. Such a possibility would imply that during this time interval of subdiffusive motion one observes a MSQD $g_1(t) \propto t^{\alpha}$ with an exponent $\alpha = 0.5$, cf. Eq. (10). We have indicated such a behavior in Fig. 5 by a dashed line with slope 0.5 and it appears compatible with the course of $g_1(t)$ in between τ_1 and τ_R for our largest membranes $L = 30-50$. If such a diffusive regime really exists, it would underline the multiscaling character of tethered membranes [24,25]. It is clear, however, that larger micelles need to be simulated with satisfactory statistics before an unambiguous conclusion in this respect can be drawn.

IV. SUMMARY AND CONCLUSIONS

In the present work we have studied the stochastic dynamics of flat self-avoiding tethered membranes which are assumed to be completely permeable to the surrounding good solvent and are thus expected to display typical Rouse behavior. By means of extensive Monte Carlo simulations we find that the static properties of our tethered membranes are described by scaling exponents which agree very well with the appropriate theoretically predicted values. Thus the radius of gyration scales with membrane linear size L as $R_g^2 \propto L^{2\nu}$ with $\nu = 1.02 \pm 0.01$, and the membrane thickness, $\lambda_{\text{min}}^2 \propto L^{2\nu_{\text{min}}}$ with roughness exponent $\nu_{\text{min}} = 0.70 \pm 0.01$, while the membrane asphericity vanishes asymptotically as $A = \lambda_{\text{min}}^2 / \lambda_{\text{max}}^2 \propto L^{-2\nu_A}$ with $\nu_A = 0.32 \pm 0.01$.

In the regime of Rouse diffusion we find with good accuracy that the diffusion coefficient $D_N \propto N^{-1}$, as predicted, whereas the typical relaxation time of such polymerized membranes grows as $\tau_R \propto L^4$ with the linear dimension L. A comparative study, involving linear polymers too, reveals also that the diffusion coefficient of permeable self-avoiding tethered membranes, containing N segments, is three times smaller than that of linear polymer chains with the same number of segments.

Our main concern in this study, however, is with the subdiffusive motion of the membranes central segment at times $t \leq \tau_R$. Our numeric studies reveal several regimes of anomalous diffusion whereby the central node MSQD grows as $g_1 \propto t^{0.86}$ for $t \leq 1$, then $g_1 \propto t^{0.27}$ for $1 \leq t \leq \tau_1$, further, with $g_1 \propto t^{0.5}$ at time $\tau_1 \leq t \leq \tau_R$, before turning eventually to normal diffusion with $g_1 \propto t$ for $t \geq \tau_R$. We use simple scaling arguments to interpret our observation and suggest that the anomalous diffusion exponent $\alpha \approx 0.27$ which we find in agreement with recent studies [24,25] most probably reflects several particular mechanisms of membrane motion. These mechanisms involve different groups of loosely bound membrane monomers whose random hops predominantly contribute to the center-of-mass motion of the whole membrane at times when most of the inner monomers are mutually blocked by their nearest neighbors and therefore remain rather immobile. The particular geometry of the membrane sheet (e.g., square, hexagonal, or rhombic) is expected to enhance the role of either periphery, or vertex monomers, and therefore slightly modify the observed value of the anomalous exponent α according to Eqs. (14) and (15). This would explain some small deviations of our data from that of earlier measurements [24,25].

We believe that our results shed some light and provide insight into the complex dynamics of polymerized membranes. It is, however, clear that further work is needed before the nature of the membrane stochastic dynamics is definitely established and understood.

ACKNOWLEDGMENTS

The authors are indebted to the Max-Planck Institute for Polymer Research in Mainz, Germany for hospitality during the stay of one of us (A.M.) as well as for the possibility to use the computational facilities of the institute.

---

[1] G. Gompper and D. M. Kroll, J. Phys.: Condens. Matter **9**, 8795 (1997).
[2] C. F. Schmidt, K. Svoboda, N. Lei, I. B. Petsche, L. E. Berman, C. R. Safinya, and G. S. Grest, Science **259**, 952 (1993).
[3] T. Hwa, E. Kokufuta, and T. Tanaka, Phys. Rev. A **44**, R2235 (1991).
[4] M. S. Spector, E. Naranjo, S. Chiruvolu, and J. A. Zasadzinski, Phys. Rev. Lett. **73**, 2867 (1994).
[5] A. Sinsawat, K. L. Anderson, R. A. Vaia, and B. L. Farmer, J. Polym. Sci., Part B: Polym. Phys **41**, 3272 (2003).
[6] *Polymer Nanocomposites, Synthesis, Characterization, and Modeling*, edited by R. Krishnamoorti and R. A. Vaia, ACS Symposium Series 804 (ACS, Washington, DC, 2002).
[7] Y. Kantor, M. Kardar, and D. R. Nelson, Phys. Rev. A **35**, 3056 (1987).
[8] P. Le Doussal, J. Phys. A **25**, L469 (1992).
[9] D. Liu and M. Plischke, Phys. Rev. A **45**, 7139 (1992).
[10] Y. Kantor and K. Kremer, Phys. Rev. E **48**, 2490 (1993).
[11] L. Radzihovsky and J. Toner, Phys. Rev. Lett. **75**, 4752 (1995).
[12] M. Plischke and D. Boal, Phys. Rev. A **38**, 4943 (1988).
[13] D. Boal, E. Levinson, D. Liu, and M. Plischke, Phys. Rev. A **40**, 3292 (1989).
[14] F. F. Abraham, W. E. Rudge, and M. Plischke, Phys. Rev. Lett. **62**, 1757 (1989).
[15] C. Münkel and D. W. Heermann, Phys. Rev. Lett. **75**, 1666 (1995).
[16] S. Mori and S. Komura, J. Phys. A **29**, 7439 (1996).
[17] B. Y. Drovetsky, J. C. Chu, and C. H. Mak, J. Chem. Phys. **108**, 6554 (1998).
[18] J.-Ph. Kownacki and H. T. Diep, Phys. Rev. E **66**, 066105 (2002).
[19] H. Koibuchi, Z. Sasaki, and K. Shinohara, Phys. Rev. E **70**, 066144 (2004).
[20] G. S. Grest and I. B. Petsche, Phys. Rev. E **50**, R1737 (1994).
[21] G. Gompper and D. M. Kroll, J. Phys.: Condens. Matter **12**, A29 (2000).
[22] E. Frey and D. R. Nelson, J. Phys. I **1**, 1715 (1991).
[23] K. J. Wiese, Eur. Phys. J. B **1**, 269 (1998).
[24] R. B. Pandey, K. L. Anderson, and B. L. Farmer, Phys. Rev. E **75**, 061913 (2007).
[25] R. B. Pandey, K. L. Anderson, H. Heinz, and B. L. Farmer, J. Polym. Sci., Part B: Polym. Phys. **43**, 1041 (2005); **43**, 3478 (2005); **44**, 2512 (2006).
[26] R. B. Bird, C. F. Curtiss, R. C. Armstrong, and O. Hassager, *Dynamics of Polymeric Liquids*, 2nd ed. (Wiley, New York, 1987), Vol. 2.
[27] H. Popova and A. Milchev, J. Chem. Phys. **127**, 194903 (2007).
[28] K. Binder, A. Milchev, and J. Baschnagel, Annu. Rev. Mater. Sci. **26**, 107 (1996).